Cellular Microbiology (2014) **16**(3), 311–323
doi:10.1111/cmi.12226
First published online 6 November 2013

Two distinct sensing pathways allow recognition of *Klebsiella pneumoniae* by *Dictyostelium* amoebae

Wanessa C. Lima,[1]* Damien Balestrino,[2] Christiane Forestier[2] and Pierre Cosson[1]
[1]*Department for Cell Physiology and Metabolism, Centre Medical Universitaire, University of Geneva, 1 rue Michel Servet, 1211 Geneva 4, Switzerland.*
[2]*Laboratoire Microorganismes: Génome et Environnement (LMGE) UMR CNRS 6023, Faculté de Pharmacie, Clermont Université, 28 place Henri Dunant, 63001 Clermont-Ferrand, France.*

Summary

Recognition of bacteria by metazoans is mediated by receptors that recognize different types of microorganisms and elicit specific cellular responses. The soil amoebae *Dictyostelium discoideum* feeds upon a variable mixture of environmental bacteria, and it is expected to recognize and adapt to various food sources. To date, however, no bacteria-sensing mechanisms have been described. In this study, we isolated a *Dictyostelium* mutant (*fspA* KO) unable to grow in the presence of non-capsulated *Klebsiella pneumoniae* bacteria, but growing as efficiently as wild-type cells in the presence of other bacteria, such as *Bacillus subtilis*. *fspA* KO cells were also unable to respond to *K. pneumoniae* and more specifically to bacterially secreted folate in a chemokinetic assay, while they responded readily to *B. subtilis.* Remarkably, both WT and *fspA* KO cells were able to grow in the presence of capsulated LM21 *K. pneumoniae*, and responded to purified capsule, indicating that capsule recognition may represent an alternative, FspA-independent mechanism for *K. pneumoniae* sensing. When LM21 capsule synthesis genes were deleted, growth and chemokinetic response were lost for *fspA* KO cells, but not for WT cells. Altogether, these results indicate that *Dictyostelium* amoebae use specific recognition mechanisms to respond to different *K. pneumoniae* elements.

Received 31 July, 2013; revised 24 September, 2013; accepted 7 October, 2013. *For correspondence. E-mail wanessa.delima@unige.ch; Tel. (+41) 22 379 5294; Fax (+41) 22 379 5260.

Introduction

In multicellular organisms, recognition of bacterial pathogens is essential to stimulate specific antibacterial responses and to allow the defence of the organism against infections. Mammalian and *Drosophila* cells make use of a collection of receptors that directly detect molecules exposed at the surface of bacteria (e.g. cell-wall components such as lipopolysaccharides or peptidoglycans) or secreted by bacteria (e.g. exotoxins or heat shock proteins) (Flannagan *et al*., 2009). In *Drosophila melanogaster*, the search for mechanisms involved in recognition of microorganisms has notably led to the discovery and characterization of Toll receptors that were later shown to also play a key role in bacterial recognition in mammalian organisms (Leulier and Lemaitre, 2008). Toll receptors are part of a signalling pathway ultimately controlling the transcriptional activity of NF-κB like transcription factors and the production of antimicrobial peptides. Recognition of bacteria by a eukaryotic cell and subsequent cell activation can be linked to initiation of phagocytosis (as in the case of lipopolysaccharides (LPS)-recognition by CD14 receptor, which triggers bacterial uptake and induces inflammatory response; Melendez and Tay, 2008), but in many instances different receptors are involved in recognition/activation and in phagocytosis of bacteria. For example, in mammalian cells, Toll-like receptors (TLRs) recognize bacterial LPS, but phagocytosis is achieved by the Fcγ and scavenger receptors upregulated by the same TLRs (Underhill and Gantner, 2004).

While specialized phagocytic cells are essential for elimination of invading microorganisms and for clearance of dying cells in multicellular organisms, in unicellular organisms such as the amoeba *Dictyostelium discoideum* phagocytosis is the main mechanism for acquiring food (Bozzaro *et al*., 2008). *Dictyostelium* amoebae exist as single cells in the soil, where they feed phagocytically upon bacteria. The molecular mechanisms that amoebae use to bind to and to ingest microorganisms are analogous to those found in multicellular organisms (Cosson and Soldati, 2008). They notably exhibit a cellular adhesion system composed of a surface receptor presenting features of integrin beta chains and binding to talin (Cornillon *et al*., 2006). Subsequent to recognition and binding, the microorganism is internalized, and ingested bacteria are killed by exposure to the harsh environment

of the mature phagosomes, characterized by an acidic pH, the presence of proteolytic enzymes, and production of reactive oxygen species (Cosson and Soldati, 2008).

Previous studies have shown that *Dictyostelium* can be attacked by a variety of bacterial pathogens (Hilbi *et al*., 2007; Bozzaro and Eichinger, 2011; Lima *et al*., 2011; Steinert, 2011). On the other hand, when confronted with non-pathogenic bacteria such as non-virulent *Klebsiella pneumoniae* or *Bacillus subtilis*, *Dictyostelium* cells use specific molecular mechanisms to kill different bacteria (Benghezal *et al*., 2006; Lelong *et al*., 2011). In addition, large-scale transcriptional studies point to differential metabolic and signalling pathways being activated when *Dictyostelium* cells are grown in different sources of bacteria (Sillo *et al*., 2008; Nasser *et al*., 2013). It is thus likely that *Dictyostelium* recognizes various kinds of bacteria and adapts its physiology. To date, it is, however, not clear whether *Dictyostelium* amoebae simply adapt their metabolism to the nutrients that they can obtain from each bacteria, or if they specifically recognize and respond to each type of bacteria by modulating their physiology and gene expression. Several key elements allowing recognition of microorganisms in metazoans such as Toll receptors or NF-κB transcription factors are absent in *Dictyostelium*. On the other hand, some proteins like CD36 that have been shown to participate in microorganism recognition in metazoans have clear orthologues in *Dictyostelium* (Cosson and Soldati, 2008), although it remains to be seen if they play equivalent roles.

In this study we investigated if and how *Dictyostelium* cells specifically recognize bacteria and respond to their presence. Our results indicate that at least two distinct mechanisms allow recognition of *K. pneumoniae* bacteria by *Dictyostelium*, one sensing the folate produced by bacteria, the other one responding to bacterial capsule.

Results

FspA, a protein essential for Dictyostelium *growth in the presence of* Klebsiella pneumoniae

The *fspA* KO cell line described in this work was isolated from a population of random insertion *Dictyostelium* mutants based on their inability to grow on a lawn of *K. pneumoniae* bacteria. We used for this initial screen a non-pathogenic, non-capsulated laboratory strain of *K. pneumoniae* (unless otherwise specified, the abbreviation Kp is used to designate this laboratory strain). Wild-type (WT) *Dictyostelium* cells were able to ingest bacteria and to form phagocytic plaques in a lawn of *K. pneumoniae* (Fig. 1A and B). On the contrary, *fspA* KO cells grew very poorly in the presence of Kp (Fig. 1B), although they grew as well as WT cells in rich liquid medium (data not shown). The mutagenic plasmid inserted in the genome of *fspA* KO cells was recovered with its flanking regions, and the site of insertion sequenced, revealing that the *fspA* KO was caused by the insertion of the mutagenic vector 98 nucleotides downstream from the start codon of the DDB_G0277237 gene (Fig. S1).

To confirm that the phenotype of the KO cells was indeed due to this insertion in the *fspA* gene, we disrupted the gene by homologous recombination in WT cells (Fig. S1) and observed the same growth defect in three independent *fspA* KO clones, which were used for all further analysis. To further characterize *fspA* KO cells, we assessed their growth on a large array of bacteria, including representatives of both Gram-positive and Gram-negative bacteria (Fig. 1B). KO cells were able to grow on all Gram-positive bacteria tested (*Bacillus subtilis*, *Micrococcus luteus* and *Staphylococcus aureus*). They also grew on several non-pathogenic Gram-negative bacteria (*Pseudomonas aeruginosa*, *Aeromonas*

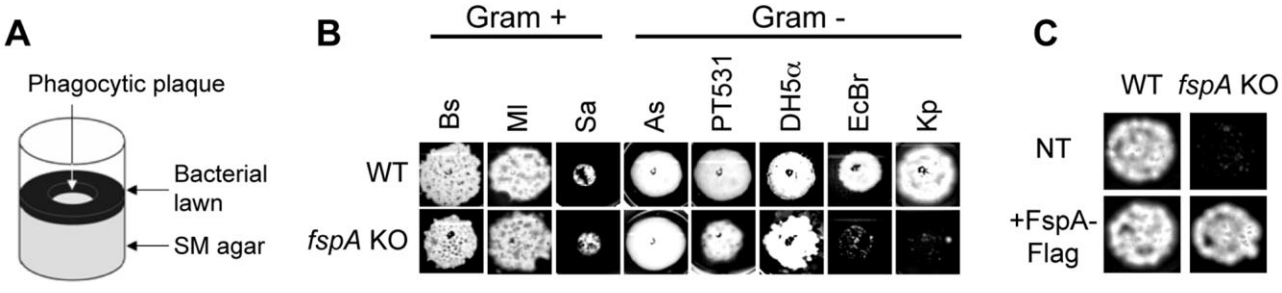

Fig. 1. *fspA* KO cells are defective for growth on *K. pneumoniae*.
A. Schematic representation of growth of *Dictyostelium* cells on a lawn of bacteria. Cells growing on bacteria form a phagocytic plaque.
B. Growth of WT and *fspA* KO cells was tested on different strains of Gram-positive and Gram-negative bacteria (described in Table S2). WT cells were able to grow on all bacteria tested. *fspA* KO cells presented a specific growth defect on some Gram-negative bacteria (*E. coli* B/r and *K. pneumoniae*), but were able to grow on all the other strains tested.
C. Complementation of *fspA* KO cells with a vector harbouring FspA cDNA restored growth on *K. pneumoniae*. NT: not transfected cells.

salmonicida, and some *Escherichia coli* strains), but not on the laboratory strain of *K. pneumoniae* or on a mucoid strain of *E. coli* (strain B/r) (Fig. 1B). Growth of *fspA* KO cells on *K. pneumoniae* bacteria was restored by introducing in the KO cells a plasmid expressing FspA tagged with a Flag epitope (Fig. 1C).

The predicted FspA protein is 333 aminoacids long, and it exhibits one putative signal peptide and potentially nine transmembrane domains (Fig. 2A). The C-terminal segment of the protein (329–332) contains a putative di-lysine ER retention motif. FspA is conserved inside the Amoebozoa group, but no clear homologues can be readily detected outside this group by primary sequence similarity searches (using BlastP at the NCBI server). However, similarity searches using AmiGO server (release GO_20130330; Carbon *et al*., 2009) revealed a weak similarity (39%) with the SRE-19 protein of *C. elegans*, a chemosensory G protein-coupled receptor (GPCR) from the nematode serpentine family (Troemel *et al*., 1995). Phylogenetic analysis was conducted using orthologues from the *C. elegans* SRE family and orthologues from rhodopsin-like olfactory receptors from diverse metazoans (identified previously as having weak similarity to the nematode genes; Sengupta *et al*., 1996). According to this analysis, amoebozoan FspA orthologues lie closer to the nematode SRE family (Fig. 2B). In addition, a search for protein domains at PROSITE webserver (Sigrist *et al*., 2010) returned a low confidence hit to GPCRs family 1 (entry PS50262, from amino acid 1 to 190). The low levels of similarity among members of the GPCR superfamily are a known feature, and classification of proteins into the group often relies on traits other than the primary sequence. Prediction of protein function using specific dedicated webservers for GPCR signature profiling (as GPCR-pred, PCA-GPCR and GPCR-CA) confirmed FspA protein as a potential putative GPCR. Collectively, these observations suggest that FspA may indeed play a role in intracellular signalling, although given the low degrees of similarity observed, their functional significance remains unclear.

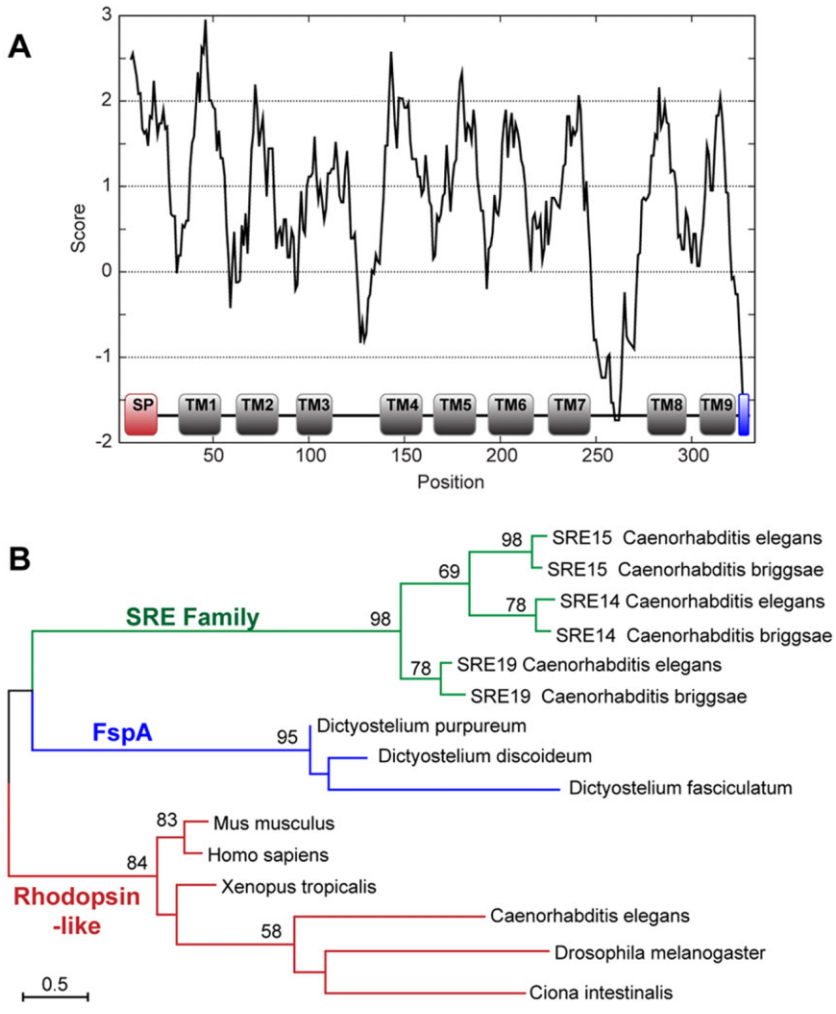

Fig. 2. FspA structure and evolutionary history.
A. Hydrophobicity plot (Kyte-Doolittle, window size of 13 residues) and predicted structure of the FspA protein. Based on primary sequence analysis, FspA exhibits a signal peptide (SP, red box) and 9 transmembrane domains (TM, grey boxes); a di-leucine ER-retention signal is present at the C-terminus (blue box).
B. Unrooted maximum likelihood tree of FspA with orthologues from nematode SRE family and metazoan rhodopsin-like olfactory receptors (refer to Table S3 for a complete list of protein accession numbers). Branch lengths are proportional to the number of amino acid substitutions per site. Numbers at the nodes represent the percentage of bootstrap support (only values > 50% are shown).

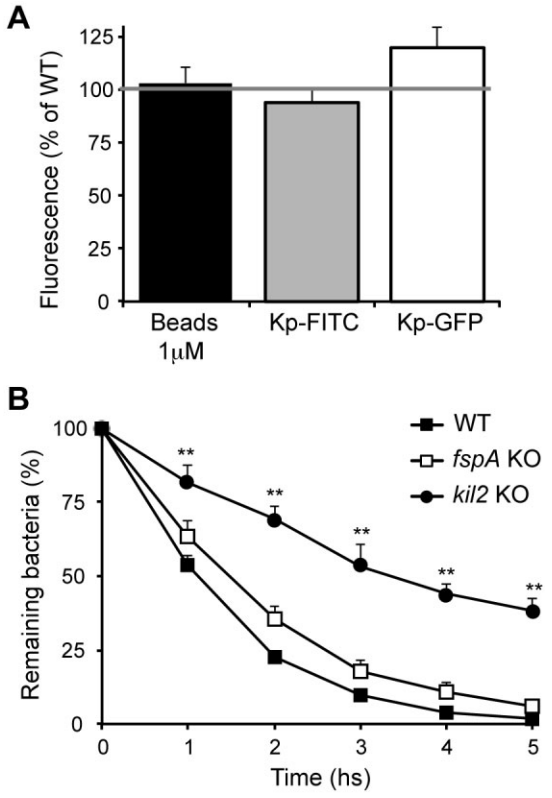

Fig. 3. *fspA* KO cells internalize and kill bacteria efficiently.
A. Internalization of 1 μm latex beads, live Kp (GFP-expressing) or dead Kp (FITC-labelled) was measured by flow cytometry. Values were normalized to 100% of WT (grey line). Phagocytosis of beads or bacteria was as efficient in *fspA* KO cells as in WT cells.
B. Killing of bacteria was assessed by mixing *Dictyostelium* (WT, *fspA* KO and the killing-defective *kil2* KO) cells and *K. pneumoniae*, and measuring the number of remaining live bacteria after different incubation times. WT cells eliminate *K. pneumoniae* rapidly, with only 25% of bacteria remaining after 2 h and less than 5% after 5 h. A similar curve was seen for the *fspA* KO cells. For comparison, *kil2* KO cells were unable to eliminate bacteria efficiently: 80% of bacteria were still alive after 2 h, and almost 40% after 5 h. $^{**}P < 0.01$, to WT values at each given time point.

fspA KO cells ingest and kill bacteria efficiently

The same defective growth observed for *fspA* KO cells, i.e. a specific inability to grow on the laboratory *K. pneumoniae* strain and on the mucoid *E. coli* B/r strain, has been previously reported for two other *Dictyostelium* KO cells unable to kill ingested *K. pneumoniae* bacteria (*phg1a* and *kil2* KO cells; Benghezal *et al*., 2006; Lelong *et al*., 2011). This led us to investigate if *fspA* KO cells can efficiently internalize and process *K. pneumoniae*. We first tested the ability of *fspA* KO cells to engulf different types of particles. Ingestion of latex beads, dead FITC-labelled or live GFP-expressing *K. pneumoniae* was not affected in *fspA* KO cells compared with WT cells (Fig. 3A), indicating that the KO cells retained their competence to ingest bacteria. *fspA* KO cells were also able to kill ingested *K. pneumoniae* bacteria as efficiently as WT cells (Fig. 3B), demonstrating that the defective growth phenotype was not linked to impaired killing.

Further characterization of the endocytic and phagocytic pathways did not reveal any other phenotypic anomaly. Notably, endosomal acidification (Fig. S2A), ingestion and recycling of fluid-phase (Fig. S2B), proteolysis of ingested substrates (Fig. S2C), and intracellular targeting of lysosomal enzymes (Fig. S2D) were not significantly different between WT and *fspA* KO cells. Together these results suggested that the inability of *fspA* KO cells to grow in the presence of *K. pneumoniae* was not caused by a defect in the function of the phagocytic pathway or in the ingestion and intracellular processing of phagocytosed bacteria.

Sensing of K. pneumoniae *and of folate is defective in fspA KO cells*

The impaired growth of *fspA* KO cells in the presence of *K. pneumoniae* could be linked to a defective recognition of the bacteria by the mutant cells. To test this, we developed a sensing assay based on the observation that WT *Dictyostelium* cells respond to the presence of different types of bacteria by significantly increasing their random migration speed (Fig. 4A). A similar method has been used previously to assess the activation state of *Dictyostelium* cells upon exposure to different compounds (Sroka *et al*., 2002; Rifkin and Goldberg, 2006). WT cells exposed to *K. pneumoniae* or to *Bacillus subtilis* bacteria migrated 2 to 3 times faster than unstimulated cells (Fig. 4B). Strikingly, in the same assay *fspA* KO cells failed to respond to the presence of *K. pneumoniae* (Fig. 4A and B), while they still reacted to *B. subtilis* (Fig. 4B).

It has been known for several years that bacteria secrete folate, which acts as a chemoattractant for *Dictyostelium* (Burkholder and McVeigh, 1942; Pan *et al*., 1972). Folate and its analogue methotrexate also act as general activators of *Dictyostelium* and can induce a variety of cellular responses, notably an increase in random cell migration in WT cells (Rifkin and Goldberg, 2006). Unlike WT cells, *fspA* KO cells did not respond to folate or to methotrexate (Fig. 4B), and this phenotype was restored in KO cells expressing FspA-Flag (Fig. 4C). To verify the specificity of this phenotype, we also assessed the ability of *kil2* KO cells to respond to *K. pneumoniae* or folate (Fig. S2E). As expected, *kil2* KO cells are able to sense both *K. pneumoniae* and folate, indicating that recognition and killing of *K. pneumoniae* are two processes involving different cellular pathways.

In order to test whether folate was a major *K. pneumoniae* factor stimulating *Dictyostelium* cells, we attempted to produce folate-depleted Kp by incubating them in the presence of sulfathiazole, an antibiotic that

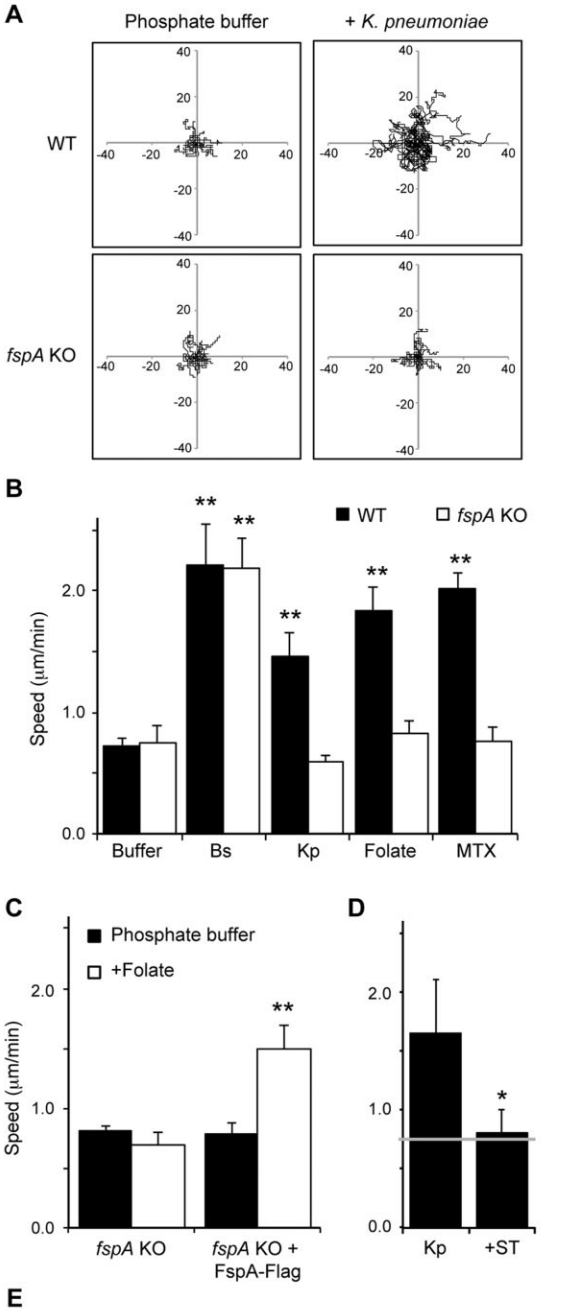

E

Gene name	GO Molecular function	Fold change WT	Fold change KO	Ratio KO/WT
grlC	G-protein coupled receptor	76.56±4.75	26.06±1.70**	34%
grlD	G-protein coupled receptor	9.40±0.47	4.05±0.37**	43%
grlM	G-protein coupled receptor	8.13±0.98	5.51±0.59*	67%

Fig. 4. Sensing of *K. pneumoniae* and folate is defective in *fspA* KO cells.
A. Trajectories of WT and *fspA* KO cells migrating for 30 min in the absence or presence of *K. pneumoniae* (the origins are set to 0). Axes represent distance in µm.
B. Average speed of WT and *fspA* KO cells in the presence of bacteria (*B. subtilis* and *K. pneumoniae*), folate and its analogue methotrexate (MTX). WT cells responded to the presence of both bacteria, while *fspA* KO cells lost the ability to sense *K. pneumoniae*. *fspA* KO cells were also impaired in the sensing of folate and MTX. $^{**}P < 0.01$, to control condition (in phosphate buffer).
C. Complementation of *fspA* KO cells with FspA restores the ability of cells to sense folate. $^{**}P < 0.01$, to *fspA* KO values.
D. *K. pneumoniae* bacteria in exponential growth phase were treated with the antibiotic sulfathiazole (ST), an inhibitor of folate biosynthesis. *K. pneumoniae* growing in the same conditions, but in the absence of antibiotics, were used as control. WT cells did not respond to folate-depleted *K. pneumoniae* (the grey line indicates speed of WT cells in phosphate buffer). $^{*}P < 0.05$, to non-treated Kp.
E. Induction of transcription upon exposure to folate is defective in *fspA* KO cells. Genes upregulated more than fourfold in WT cells upon exposure to folate (Table S1) were also analysed in *fspA* KO cells: in these cells, upregulation was not as effective as in WT cells, showing a 35–65% reduced induction. $^{*}P < 0.05$ and $^{**}P < 0.01$, to WT fold change values.

inhibits bacterial folate biosynthesis by preventing the formation of the precursor dihydropteroate (Herrington, 1994). WT *Dictyostelium* cells did not respond to folate-depleted *K. pneumoniae* (Fig. 4D), suggesting that in these conditions, *Dictyostelium* cells may respond to the presence of *K. pneumoniae* bacteria mostly through folate sensing. We named the FspA protein on the basis of its essential role in folate sensing (Folate Sensing Protein A).

To further characterize the cell response to folate in WT and *fspA* KO cells, we analysed the transcriptional response of several genes after 1 h of incubation in phosphate buffer in the presence or absence of folate. The 50 genes analysed here (Table S1) were chosen partly based on microarray studies of *Dictyostelium* cells growing in the presence of bacteria (Farbrother *et al*., 2006; Carilla-Latorre *et al*., 2008; Sillo *et al*., 2008), but also included genes potentially involved in intracellular signalling, such as GPCRs. In WT cells, only 3 genes (all coding for GPCRs) were induced more than fourfold upon exposure to folate: *grlC*, *grlD*, and *grlM* (Fig. 4E and Table S1). In *fspA* KO cells exposed to folate, the expression levels of these three genes were 35–65% lower than in WT cells (Fig. 4E). This result also points to an inefficient response of *fspA* KO cells to folate.

Dictyostelium *cells sense* K. pneumoniae *capsule in an FspA-independent manner*

The laboratory strain of *K. pneumoniae* used in this study is characterized by its lack of pathogenicity, as well as by the lack of a visible capsule (Fig. 5A and Benghezal *et al*., 2006). Measurement of capsule content also revealed no detectable capsule production (undistinguished from background values). Most clinical or environmental isolates of *K. pneumoniae* exhibit a capsule, which represents one of the key virulence factors of *K. pneumoniae* (Podschun and Ullmann, 1998). In order to check if the presence of a capsule affects interactions between

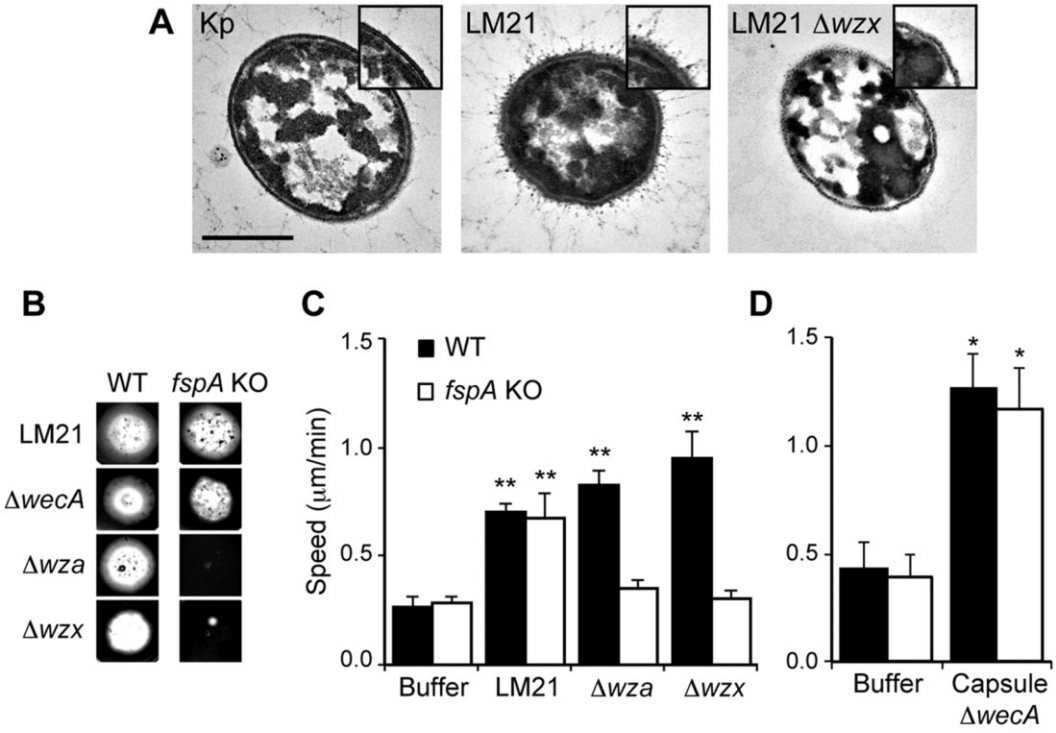

Fig. 5. An FspA-independent pathway allows sensing of *K. pneumoniae* capsule.
A. Electron micrographs of *K. pneumoniae* bacteria (laboratory Kp strain, LM21 and the LM21 capsule-defective Δ*wzx* mutant). A capsule is visible at the surface of LM21, but not of other strains. Scale bar: 0.5 μm.
B. Growth of WT and *fspA* KO cells was tested in the presence of LM21 WT or of LM21 mutants devoid of LPS (Δ*wecA*) or of capsule (Δ*wza* and Δ*wzx*). WT *Dictyostelium* cells were able to grow on all bacterial strains tested. While *fspA* KO cells grew on LM21 and on an LPS^{-} mutant, they were unable to grow on mutants devoid of capsule.
C. Average speed of WT and *fspA* KO cells in the presence of LM21 WT and capsule mutants (Δ*wza* and Δ*wzx*). *Dictyostelium* WT cells moved faster in the presence of the three bacteria tested, but *fspA* KO cells did not respond to the capsule mutants. $^{**}P < 0.01$, to control condition (phosphate buffer).
D. Average speed of WT and *fspA* KO cells in the presence of purified capsule from LM21 Δ*wecA*. Both WT and KO cells responded to capsule, as indicated by a threefold increase in speed when compared with control values. $^{*}P < 0.05$, to control condition (phosphate buffer).

K. pneumoniae and *Dictyostelium*, we tested the ability of WT and *fspA* KO cells to grow in the presence of LM21, a well-characterized capsulated strain of *K. pneumoniae* (Favre-Bonte *et al*., 1999). Surprisingly, both WT as well as *fspA* KO *Dictyostelium* cells were able to grow in the presence of LM21 (Fig. 5B).

To determine the nature of this FspA-independent growth in the presence of LM21 *K. pneumoniae*, we tested several LM21 mutant strains, impaired in the production of different exopolysaccharides, capsule and LPS. LM21 Δ*wza* and Δ*wzx*, both devoid of capsule (Fig. 5A, and Balestrino *et al*., 2008), did not support growth of *fspA* KO cells (Fig. 5B), indicating that the presence of a capsule is necessary and sufficient to allow growth of *fspA* KO cells in the presence of *K. pneumoniae*. Accordingly, both WT as *fspA* KO cells presented increased motility in the presence of LM21 *K. pneumoniae*, but only WT cells could respond to the capsule mutants (Fig. 5C). To further characterize the effect of capsule, we assessed the ability of cells to respond to purified capsule extracted from an LPS-deficient strain (LM21 Δ*wecA*): both WT and *fspA* KO cells responded to the presence of an LPS-free capsule extract (Fig. 5D).

Together these results suggest that an FspA-independent mechanism allows *Dictyostelium* to sense *K. pneumoniae* capsule, and that this activation is sufficient to support growth of *fspA* KO cells in the presence of *K. pneumoniae*.

Intracellular localization of FspA

Since Flag-tagged FspA restored a wild-type phenotype in *fspA* KO cells (Figs 1C and 4C), at least part of this tagged protein was presumably correctly localized within the cell. When assessed by immunofluorescence, the bulk of FspA-Flag appeared colocalized with PDI (Fig. 6A), a marker of the endoplasmic reticulum. No significant colocalization was seen with a marker of endosomal compartments (p80 protein; Ravanel *et al*.,

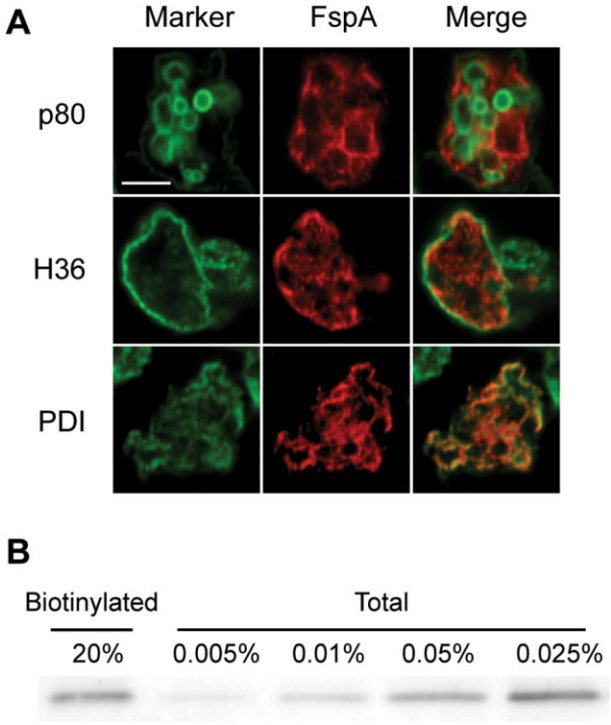

Fig. 6. FspA localizes mostly in the endoplasmic reticulum.
A. Colocalization of FspA-Flag with markers for endosomal compartments (p80), plasma membrane (H36) and endoplasmic reticulum (PDI). FspA colocalizes extensively with ER. Scale bar: 5 μm.
B. To assess the presence of FspA-Flag at the cell surface, plasma membrane proteins were biotinylated, purified on neutravidin beads, and the presence of FspA was revealed with an anti-Flag antibody in the total cell lysate and in the biotinylated protein fraction. The Western blot of a representative experiment is shown; all lanes are from the same gel and have the same exposure time. 20% of the total biotinylated fraction volume was loaded, and dilutions of the lysate (from 0.025% to 0.005% of the total lysate volume) were used to estimate the amount of biotinylated proteins. Only a very small fraction of the FspA protein was detected at the cell surface (< 1%). However, as a measure of background, a 5- to 10-fold lower fraction was detected at the cell surface for two negative controls: a cytoplasmic protein (actin) or an ER-resident protein (PDI) (Fig. S3).

2001), contractile vacuole (Rhesus protein; Benghezal *et al*., 2001), or plasma membrane (H36) (Fig. 6A).

However, we could not exclude based on immunofluorescence that a small fraction of FspA might be present at the cell surface. In order to investigate this point, the surface of intact cells was biotinylated and the presence of FspA-Flag was assessed among the purified biotinylated proteins. A small fraction of the FspA protein was biotinylated, corresponding to less than 1% of the total protein (Fig. 6B). This was however higher (5- to 10-fold) than detected for a cytosolic protein (actin) or a resident ER protein (PDI) (Fig. S3). This result suggests that, while a major part of FspA localizes in the ER, a fraction of it may be present at the cell surface. This surface localization of FspA is however tentative, since accidental rupture of a few cells during biotinylation can result in artefactual biotinylation of a small percentage of intracellular proteins.

Discussion

Dictyostelium *sensing of bacterial-secreted folate*

In metazoan organisms, recognition of pathogens is mostly mediated by cellular receptors that detect bacterial components and trigger specific signal transduction pathways. Environmental amoebae, such as *Dictyostelium discoideum*, rely on bacteria present on the soil as food source. To achieve this aim they must forage, internalize, kill and digest bacteria. *Dictyostelium* is able to grow on many different types of bacteria, and specific transcriptional responses have been observed in different conditions (Farbrother *et al*., 2006; Carilla-Latorre *et al*., 2008; Sillo *et al*., 2008; Nasser *et al*., 2013). However, most of these studies analysed steady-state situations, and to date it is still not clear if *Dictyostelium* specifically recognizes different types of bacteria and triggers defined adaptation pathways, or if the specific response occurs at a metabolic level, as an *a posteriori* adaptation to the different intracellular levels of available metabolites. In this study, we show that at least two distinct signalling pathways allow recognition of *K. pneumoniae* by *Dictyostelium* cells: one involves sensing of bacterial capsule, while the other relies on the detection of folate secreted by the bacteria (Fig. 7).

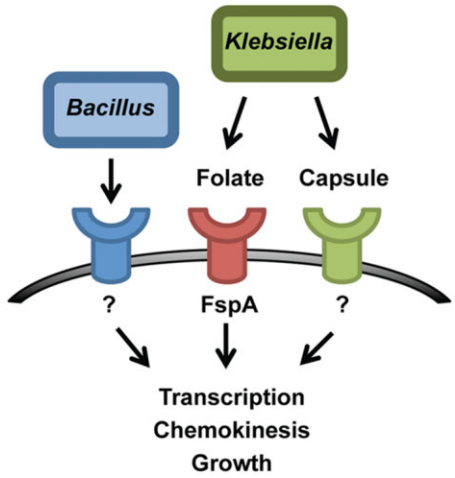

Fig. 7. Distinct pathways allow *Dictyostelium* amoebae to recognize bacteria. Our results suggest that *Dictyostelium* cells are able to recognize *K. pneumoniae* bacteria through at least two distinct pathways, one sensing bacterial capsule, and the other sensing folate. The FspA protein is an essential component of the folate-sensing pathway, but it does not play a role in capsule sensing. Recognition of bacterial components leads to different cellular responses: transcriptional regulation, motility and growth. At least one additional mechanism must be at play for the recognition of other bacteria like the Gram-positive *Bacillus subtilis*.

The isolation and characterization of *fspA* KO cells allowed us to show that, in order to grow in the presence of *K. pneumoniae*, *Dictyostelium* must specifically recognize these bacteria. When *Dictyostelium* is exposed to a laboratory, non-capsulated strain of *K. pneumoniae*, the sole activation pathway at play involves sensing of folate secreted by bacteria, and the FspA protein is an essential element for the activation of this pathway. The FspA-dependent folate-sensing pathway regulates the immediate response of *Dictyostelium* to folate (chemokinetic responses), a rapid transcriptional response (within 1 h of exposure), and it is essential for sustained growth in the presence of bacteria. Note that, when analysing transcriptional responses, we focused on relatively short-term responses (1 h), and it thus seems likely that we are measuring the primary response of *Dictyostelium* to folate, rather than a long-term adaptation process. This is in stark difference to most published studies that analysed cell response to bacteria after longer exposure times (from 2 h to 14 h or more) (Carilla-Latorre *et al*., 2008; Sillo *et al*., 2008; Nasser *et al*., 2013), and may account for the fact that none of the genes identified in these previous studies was upregulated upon short exposure to folate.

To date, our results do not allow us to define the exact role of FspA in folate sensing. Based on the phenotype of *fspA* KO cells, FspA may act as a folate receptor acting either at the cell surface or in the endoplasmic reticulum, where we detected most of the Flag-tagged FspA protein. This would be compatible with the observation that FspA is a polytopic membrane protein homologous to *C. elegans* GPCR chemosensory receptors (Fig. 2). Alternatively FspA may represent another essential element in the folate-sensing pathway, acting either as a regulator of another, unidentified, receptor, or in the regulation of the intracellular signal relay. It is known that the response of *Dictyostelium* cells to folate induces increases in cGMP content, indicating that the response is modulated by heterotrimeric G proteins, notably via Gα4 (Kesbeke *et al*., 1990; Hadwiger *et al*., 1994). Transcriptional response to folate includes a strong induction of a few GPCRs (Table S1), and FspA is partially involved in this response. FspA might be a first-line signal transducer, further activating other GPCR proteins also capable of sensing folate.

It is also worth noting the striking phenotypic similarity between *fspA* KO cells and two other KO cells previously isolated in our laboratory, the killing-deficient mutants *kil2* and *phg1a* KO cells. The three cell lines have a very specific defective growth on *E. coli* B/r and the laboratory *K. pneumoniae* strain, but as discussed above the molecular mechanisms mediating growth impairment are different. This suggests the existence of a *Klebsiella*-adaptation module, in which FspA, Kil2 and Phg1A play different roles in sensing and killing.

Dictyostelium *sensing of bacterial capsule*

Our results imply that folate sensing is critical for sustained growth of *Dictyostelium* in the presence of a laboratory, non-capsulated strain of *K. pneumoniae*. However, *fspA* KO cells grew efficiently in the presence of LM21, a capsulated strain of *K. pneumoniae.* Analysis of LM21 mutants indicates that the presence of a capsule makes LM21 permissive for growth of *fspA* KO cells. The fact that *fspA* KO cells are unable to grow on, and also unable to respond to, capsule-deficient bacteria (as the Kp laboratory strain and LM21 Δ*wza* and Δ*wzx* mutants) points to a dual recognition mechanism of *K. pneumoniae* by *Dictyostelium*: in the absence of capsule, *Dictyostelium* relies solely on folate sensing for detecting bacteria, and this recognition is mediated via FspA. On the other hand, recognition of capsule is achieved by an alternative FspA-independent pathway (Fig. 7).

In *K. pneumoniae*, the capsule is one of the key virulence determinants, and it is often related to reduced ability of mammalian host cells to phagocyte bacteria (Podschun and Ullmann, 1998; Cortes *et al*., 2002; Evrard *et al*., 2010). In *Dictyostelium* amoebae, capsule-defective mutants of the capsulated Kp52145 were also killed more efficiently than the corresponding WT bacteria (March *et al*., 2013). When comparing the ability of *Dictyostelium* cells to grow on the capsulated LM21 strain or on its isogenic capsule mutants, WT *Dictyostelium* cells grew faster on the latter: it took 5–6 days for WT *Dictyostelium* to form a phagocytosis plaque on WT *K. pneumoniae*, but only 2–3 days on capsule-defective bacteria. This observation indicates that bacterial capsule plays a dual role in the interaction between *K. pneumoniae* and *Dictyostelium*: on the one hand it increases resistance of bacteria to intracellular phagocytosis and killing; on the other hand *Dictyostelium* has evolved a recognition system that allows it to sense the capsule and to modulate its response when facing these bacteria. Further genetic screens will be necessary to identify FspA-independent mechanisms allowing sensing of *K. pneumoniae* capsule or of Gram-positive bacteria.

Altogether, these results indicate that amoeba cells use a variety of mechanisms to sense different bacterial components and to grow in the presence of bacteria (Fig. 7). This is in accordance with the ecological niche that amoebae occupy: given the diversity of available food in the soil, cells should be able to recognize different bacterial components and to respond accordingly. Although previous studies, focused on transcriptional changes, already highlighted how the metabolism of amoebae adapts to different food sources (Carilla-Latorre *et al*., 2008; Sillo *et al*., 2008; Nasser *et al*., 2013), this study goes one step further with the identification of the molecular pathways involved on bacterial recognition.

Experimental procedures

Screening for growth-deficient Dictyostelium *mutants*

Mutants unable to grow on a laboratory strain of *Klebsiella pneumoniae* (Kp; Benghezal *et al*., 2006) bacteria were selected by restriction enzyme-mediated integration (REMI) mutagenesis (Kuspa, 2006) as described previously (Cornillon *et al*., 2000; Lelong *et al*., 2011). Mutants in which the plasmid insertion was in a coding region were selected, re-transfected with the recovered knockout plasmid (Fig. S1) and analysed again for defective growth. One mutant (herein denominated *fspA*) proved to be defective after this second screening round and was selected for further characterization.

Cell culture, plasmids and bacterial strains

All *Dictyostelium* strains used in this study were derived from the subclone DH1–10 (Cornillon *et al*., 2000) of the DH1 strain, referred to as wild-type for simplicity. Cells were grown at 21°C in HL5 medium and subcultured twice a week to maintain a maximal density of 10^6 cells ml^{-1}.

A knockout vector was obtained during the mutagenesis, consisting of the REMI vector flanked by genomic regions comprising *fspA* gene (Fig. S1). The ClaI-digested plasmid was introduced into WT cells by electroporation, transfected cells were selected in the presence of 10 μg ml^{-1} blasticidin, and individual clones were screened by PCR (Fig. S1E). Three independent KO clones were generated and analysed in this study, and presented identical phenotypes.

An expression vector carrying a tagged version of the *fspA* gene was constructed by introducing a C-terminal Flag epitope (DYKDDDDK) into the FspA cDNA coding sequence and transfected in WT and *fspA* KO cells by electroporation; transfected cells were selected in the presence of 10 μg ml^{-1} G418.

The full list of bacterial strains used in this study is presented in Table S2. In all experiments, bacteria were grown in SM medium (10 g l^{-1} bacteriological peptone, 1 g l^{-1} yeast extract, 16.2 mM KH_2PO_4, 5.7 mM K_2HPO_4 and 4 mM $MgSO_4$) supplemented with 1% glucose. For the study of bacteria morphology by electron microscopy, bacteria were fixed in 2% glutaraldehyde (1 h at room temperature) and post-fixed in 2% osmium tetroxide (1 h at 4°C), dehydrated and embedded in Epon resin and processed for conventional electron microscopy as previously described (Marchetti *et al*., 2004).

For capsule quantification, capsular polysaccharides were extracted from an overnight bacterial culture growing in DW medium (a defined medium designed for optimal capsule production) and quantified by measuring uronic acid concentration (compared with a standard curve of D-glucuronic acid) (Domenico *et al*., 1989; Balestrino *et al*., 2008). To produce folate-depleted *K. pneumoniae*, cells growing in exponential phase (OD 0.3–0.4) were washed twice in phosphate buffer and incubated for 2 h with 250 μg ml^{-1} sulfathiazole (Sigma-Aldrich).

Growth of Dictyostelium *on bacteria and intracellular killing*

The procedure to test growth of *Dictyostelium* cells on a bacterial lawn has been described previously (Froquet *et al*., 2009). Briefly, 10^3 *Dictyostelium* cells were deposited on a bacterial lawn (50 μl of an overnight culture) and allowed to grow until the WT cells form a phagocytic plaque. The number of days for such depends on the bacteria tested: Bs (4 days), Ml (4), Sa (4), As (2), PT531 (4), DH5α (2), EcBr (3), Kp (3), LM21 (5), LM21 Δ*wza* (2), LM21 Δ*wzx* (3), and LM21 Δ*wecA* (5).

Killing of bacteria was also assessed as described previously (Lelong *et al*., 2011). Briefly, 2×10^6 *Dictyostelium* cells were mixed with 2×10^4 Kp bacteria, and incubated at 21°C for up to 5 h. After 0, 1, 2, 3, 4 or 5 h of incubation, a 10 μl aliquot of the suspension was collected and diluted in 100 μl of 0.1% Triton X-100, plated in LB agar and the number of colonies counted to assess the number of live bacteria remaining.

Chemokinetic assay

For chemokinetic measurements, 5×10^5 *Dictyostelium* cells were allowed to attach on glass bottom 35 mm fluorodishes (WPI, World Precision Instruments, Sarasota, FL) for 20 min in phosphate buffer (2 mM Na_2HPO_4, 14.7 mM KH_2PO_4, pH 6.0) with or without addition of folate or methotrexate (2 mM), purified capsule (1 μg ml^{-1}) or bacteria (1:100 v/v., from an overnight culture washed twice in phosphate buffer). Cells were then imaged for 30 min (pictures every 15 s) in a wide-field inverted Zeiss Axiovert 100 M, with a Plan-Neofluar 10× objective. The time series images were acquired with a Hamamatsu CCD cooled camera and assembled into a movie using Metamorph (Molecular Devices, Sunnyvale, CA). Particle tracking application for Metamorph was used to track the individual trajectories and total distance of at least 15 cells per experiment.

Endocytic pathway assessment

The internalization of phagocytic particles was measured as follows: 10^5 cells were incubated at 21°C in HL5 medium containing 1 μl ml^{-1} of 1 μm diameter FITC-fluorescent latex beads (Polysciences, Warrington, PA) or 10^7 fluorescent Kp (either live-GFP-labelled or dead-FITC-labelled), harvested after 30 min, washed with ice-cold HL5 containing 0.1% sodium azide, and analysed by flow cytometry (FACS Calibur, Beckton Dickinson, San Jose, CA).

Endosomal pH was measured by flow cytometry as described previously (Marchetti *et al*., 2009). The activity of lysosomal enzymes was measured using a colorimetric assay (Froquet *et al*., 2008) and the kinetics of phagosomal proteolytic activity using the un-quenching of DQ Green BSA-tagged beads (Sattler *et al*., 2013).

Fluorescence microscopy

To perform immunofluorescence, 10^6 cells were incubated on a glass coverslip for 3 h at 21°C, fixed in 4% paraformaldehyde, permeabilized with 0.07% Triton X-100 and labelled as already described (Charette *et al*., 2006). Cells were visualized with an LSM700 confocal microscope (Carl Zeiss). Mouse monoclonal antibodies against the endosomal marker p80 (H161) and the plasma membrane protein H36 and a rabbit antiserum against the contractile vacuole marker Rh were described previously (Benghezal *et al*., 2001; Ravanel *et al*., 2001; Mercanti *et al*., 2006). Endoplasmic reticulum marker PDI (protein disulfide

isomerase) was detected using 221-64-1, a mouse monoclonal antibody (Monnat *et al*., 1997). Mouse monoclonal anti-Flag antibody (clone M2) was from Sigma-Aldrich, and fluorescent secondary goat anti-mouse or anti-rabbit IgG from Molecular Probes.

Surface biotinylation

To detect biotinylated FspA-Flag at the cell surface, 3×10^7 cells were washed twice in ice-cold phosphate buffer containing 120 mM sorbitol (pH 6.0), resuspended and incubated for 10 min in ice-cold phosphate buffer with 120 mM sorbitol (pH 8.0) containing 0.5 mg ml^{-1} sulfo-NHS-SS-biotin (Thermo Scientific, Rockford, IL), then washed once in phosphate buffer containing 100 mM glycine and 4 times in phosphate buffer containing 120 mM sorbitol (pH 6.0). Cells were lysed 15 min in lysis buffer (50 mM Tris pH 7.4, 150 mM NaCl, 1% Triton X-100, 1% sodium deoxycholate) containing protease inhibitors (2 mg ml^{-1} iodoacetamide, 2 μg ml^{-1} phenylmethylsulfonylfluoride, 1 μg ml^{-1} aprotinin, and 2 μg ml^{-1} leupeptin), and the supernatant was incubated overnight with Neutravidin Ultralink beads (Thermo Scientific, Rockford, IL). Beads were incubated 15 min in 6 M urea, washed 3 times in lysis buffer, heated at 60°C, and the eluate resuspended in 2× sample buffer (0.6 M sucrose, 0.1 M Tris pH 6.8, 10 mM EDTA pH 8.0, 1 mg ml^{-1} bromophenol blue, 4% SDS). Biotinylated proteins were separated on a 12% SDS-PAGE gel, transferred to nitrocellulose membranes, detected with a primary mouse anti-Flag antibody (Sigma-Aldrich) and a secondary HRP-coupled goat anti-mouse IgG (Bio-Rad, Hercules, CA) and revealed using a chemiluminescence imager (PXi Syngene, Cambridge, UK). As a positive control, a cell surface protein (SibA; Cornillon *et al*., 2006) was analysed. Cytoplasmic actin and ER-resident PDI (protein disulfide isomerase, Monnat *et al*., 1997) were used as negative controls.

RT-PCR

5×10^6 *Dictyostelium* cells were incubated for 1 h in phosphate buffer with or without addition of 2 mM folate. Cells were then harvested and RNAs purified with a Qiagen RNeasy kit. cDNA was synthesized from 1 μg of total RNA using random hexamers and Superscript II reverse transcriptase (Invitrogen). Amplicons (50 to 100 bp) were designed using the program PrimerQuest (Integrated DNA Technologies, Coralville, IO) with parameters adjusted for GC content (40%) and maximum T_M difference (1°C). Oligonucleotide sequences were aligned against the *Dictyostelium* coding sequence database by BLAST to ensure that they were specific for the gene tested. Oligonucleotides were obtained from Invitrogen, and Table S1 shows a list of all genes analysed. PCR reactions (14 μl) contained SYBR Green Master Mix (Applied Biosystems), diluted cDNA (1 ng) and 500 nM of forward and reverse primers, and were analysed in a StepOnePlus cycler (Invitrogen) with the following parameters: 95°C for 20 s, 40 cycles of 95°C/3 s and 60°C/30 s. Raw C_T values were imported into Excel (Microsoft Corporation), and fold changes were calculated as $2^{-\Delta(\Delta C_T)}$, where $\Delta C_T = C_T$ (target) $- C_T$ (control genes: *act* and *rnl*) and $\Delta(\Delta C_T) = \Delta C_T$ (stimulated: 1 h in the presence of folate) $- \Delta C_T$ (control condition: 1 h without folate).

Sequence and phylogenetic analysis

Sequence similarity analyses were performed using BlastP program against the protein databases deposited at NCBI, AmiGO and DictyBase servers (Johnson *et al*., 2008; Carbon *et al*., 2009; Fey *et al*., 2009). Signal peptide and transmembrane domains were detected using, respectively, SignalP and TMHMM (Krogh *et al*., 2001; Petersen *et al*., 2011). Protein domains and motifs were scanned using InterPro and PROSITE (Hunter *et al*., 2012; Sigrist *et al*., 2013), and prediction of primary sequences as GPCR proteins done via GPCR-pred (Bhasin and Raghava, 2004), PCA-GPCR (Peng *et al*., 2010) and GPCR-CA (Xiao *et al*., 2009) webservers. For phylogenetic analyses, protein sequences were aligned with CLUSTALX 2.0 program (Larkin *et al*., 2007). Maximum likelihood trees were computed by using MEGA 5.0 (Tamura *et al*., 2011), with the WAG+F model, and parameters for invariable sites and gamma-distributed rate heterogeneity (5 categories). One hundred bootstrap replicates were executed and bootstrap values drawn up on the consensus ML-tree.

Statistical analysis

Unless otherwise specified, for quantified data, the values represent the arithmetical mean and s.e.m. of at least three independent experiments. Statistical comparisons were done with Student's *t*-tests (two-tailed, unpaired).

Acknowledgements

We thank the personal from the Pôle Facultaire de Microscopie Ultrastructurale (PFMU) of the University of Geneva for the preparation of the electron micrograph samples. We also thank Thierry Soldati laboratory for providing the DQ Green BSA-tagged beads. PC laboratory is funded by a grant from the Swiss National Science Foundation (number 31003A-135789), and WCL was partially supported by a Téléthon Action Suisse grant.

Conflict of interest

The authors declare that they have no conflict of interest.

References

Balestrino, D., Ghigo, J.M., Charbonnel, N., Haagensen, J.A., and Forestier, C. (2008) The characterization of functions involved in the establishment and maturation of *Klebsiella pneumoniae* in vitro biofilm reveals dual roles for surface exopolysaccharides. *Environ Microbiol* **10:** 685–701.

Benghezal, M., Gotthardt, D., Cornillon, S., and Cosson, P. (2001) Localization of the Rh50-like protein to the contractile vacuole in *Dictyostelium*. *Immunogenetics* **52:** 284–288.

Benghezal, M., Fauvarque, M.O., Tournebize, R., Froquet, R., Marchetti, A., Bergeret, E., *et al*. (2006) Specific host genes required for the killing of *Klebsiella* bacteria by phagocytes. *Cell Microbiol* **8:** 139–148.

Bhasin, M., and Raghava, G.P. (2004) GPCRpred: an SVM-based method for prediction of families and subfamilies of G-protein coupled receptors. *Nucleic Acids Res* **32:** W383–W389.

Bozzaro, S., and Eichinger, L. (2011) The professional phagocyte *Dictyostelium discoideum* as a model host for bacterial pathogens. *Curr Drug Targets* **12:** 942–954.

Bozzaro, S., Bucci, C., and Steinert, M. (2008) Phagocytosis and host-pathogen interactions in *Dictyostelium* with a look at macrophages. *Int Rev Cell Mol Biol* **271:** 253–300.

Burkholder, P.R., and McVeigh, I. (1942) Synthesis of vitamins by intestinal bacteria. *Proc Natl Acad Sci USA* **28:** 285–289.

Carbon, S., Ireland, A., Mungall, C.J., Shu, S., Marshall, B., and Lewis, S. (2009) AmiGO: online access to ontology and annotation data. *Bioinformatics* **25:** 288–289.

Carilla-Latorre, S., Calvo-Garrido, J., Bloomfield, G., Skelton, J., Kay, R.R., Ivens, A., *et al*. (2008) *Dictyostelium* transcriptional responses to *Pseudomonas aeruginosa*: common and specific effects from PAO1 and PA14 strains. *BMC Microbiol* **8:** 109.

Charette, S.J., Mercanti, V., Letourneur, F., Bennett, N., and Cosson, P. (2006) A role for adaptor protein-3 complex in the organization of the endocytic pathway in *Dictyostelium*. *Traffic* **7:** 1528–1538.

Cornillon, S., Pech, E., Benghezal, M., Ravanel, K., Gaynor, E., Letourneur, F., *et al*. (2000) Phg1p is a nine-transmembrane protein superfamily member involved in dictyostelium adhesion and phagocytosis. *J Biol Chem* **275:** 34287–34292.

Cornillon, S., Gebbie, L., Benghezal, M., Nair, P., Keller, S., Wehrle-Haller, B., *et al*. (2006) An adhesion molecule in free-living *Dictyostelium* amoebae with integrin beta features. *EMBO Rep* **7:** 617–621.

Cortes, G., Borrell, N., de Astorza, B., Gomez, C., Sauleda, J., and Alberti, S. (2002) Molecular analysis of the contribution of the capsular polysaccharide and the lipopolysaccharide O side chain to the virulence of *Klebsiella pneumoniae* in a murine model of pneumonia. *Infect Immun* **70:** 2583–2590.

Cosson, P., and Soldati, T. (2008) Eat, kill or die: when amoeba meets bacteria. *Curr Opin Microbiol* **11:** 271–276.

Domenico, P., Schwartz, S., and Cunha, B.A. (1989) Reduction of capsular polysaccharide production in *Klebsiella pneumoniae* by sodium salicylate. *Infect Immun* **57:** 3778–3782.

Evrard, B., Balestrino, D., Dosgilbert, A., Bouya-Gachancard, J.L., Charbonnel, N., Forestier, C., and Tridon, A. (2010) Roles of capsule and lipopolysaccharide O antigen in interactions of human monocyte-derived dendritic cells and *Klebsiella pneumoniae*. *Infect Immun* **78:** 210–219.

Farbrother, P., Wagner, C., Na, J., Tunggal, B., Morio, T., Urushihara, H., *et al*. (2006) *Dictyostelium* transcriptional host cell response upon infection with *Legionella*. *Cell Microbiol* **8:** 438–456.

Favre-Bonte, S., Joly, B., and Forestier, C. (1999) Consequences of reduction of *Klebsiella pneumoniae* capsule expression on interactions of this bacterium with epithelial cells. *Infect Immun* **67:** 554–561.

Fey, P., Gaudet, P., Curk, T., Zupan, B., Just, E.M., Basu, S., *et al*. (2009) dictyBase: a *Dictyostelium* bioinformatics resource update. *Nucleic Acids Res* **37:** D515–D519.

Flannagan, R.S., Cosio, G., and Grinstein, S. (2009) Antimicrobial mechanisms of phagocytes and bacterial evasion strategies. *Nat Rev Microbiol* **7:** 355–366.

Froquet, R., Cherix, N., Birke, R., Benghezal, M., Cameroni, E., Letourneur, F., *et al*. (2008) Control of cellular physiology by TM9 proteins in yeast and *Dictyostelium*. *J Biol Chem* **283:** 6764–6772.

Froquet, R., Lelong, E., Marchetti, A., and Cosson, P. (2009) *Dictyostelium discoideum*: a model host to measure bacterial virulence. *Nat Protoc* **4:** 25–30.

Hadwiger, J.A., Lee, S., and Firtel, R.A. (1994) The G alpha subunit G alpha 4 couples to pterin receptors and identifies a signaling pathway that is essential for multicellular development in *Dictyostelium*. *Proc Natl Acad Sci USA* **91:** 10566–10570.

Herrington, M.B. (1994) Measurement of the uptake of radioactive para-aminobenzoic acid monitors folate biosynthesis in *Escherichia coli* K-12. *Anal Biochem* **216:** 427–430.

Hilbi, H., Weber, S.S., Ragaz, C., Nyfeler, Y., and Urwyler, S. (2007) Environmental predators as models for bacterial pathogenesis. *Environ Microbiol* **9:** 563–575.

Hunter, S., Jones, P., Mitchell, A., Apweiler, R., Attwood, T.K., Bateman, A., *et al*. (2012) InterPro in 2011: new developments in the family and domain prediction database. *Nucleic Acids Res* **40:** D306–D312.

Johnson, M., Zaretskaya, I., Raytselis, Y., Merezhuk, Y., McGinnis, S., and Madden, T.L. (2008) NCBI BLAST: a better web interface. *Nucleic Acids Res* **36:** W5–W9.

Kesbeke, F., Van Haastert, P.J.M., De Wit, R.J.W., and Snaar-Jagalska, B.E. (1990) Chemotaxis to cyclic AMP and folic acid is mediated by different G proteins in *Dictyostelium discoideum*. *J Cell Sci* **96:** 669–673.

Krogh, A., Larsson, B., von Heijne, G., and Sonnhammer, E.L. (2001) Predicting transmembrane protein topology with a hidden Markov model: application to complete genomes. *J Mol Biol* **305:** 567–580.

Kuspa, A. (2006) Restriction enzyme-mediated integration (REMI) mutagenesis. *Methods Mol Biol* **346:** 201–209.

Larkin, M.A., Blackshields, G., Brown, N.P., Chenna, R., McGettigan, P.A., McWilliam, H., *et al*. (2007) Clustal W and Clustal X version 2.0. *Bioinformatics* **23:** 2947–2948. PMID: 17846036.

Lelong, E., Marchetti, A., Gueho, A., Lima, W.C., Sattler, N., Molmeret, M., *et al*. (2011) Role of magnesium and a phagosomal P-type ATPase in intracellular bacterial killing. *Cell Microbiol* **13:** 246–258.

Leulier, F., and Lemaitre, B. (2008) Toll-like receptors: taking an evolutionary approach. *Nat Rev Genet* **9:** 165–178.

Lima, W.C., Lelong, E., and Cosson, P. (2011) What can *Dictyostelium* bring to the study of *Pseudomonas* infections? *Semin Cell Dev Biol* **22:** 77–81.

March, C., Cano, V., Moranta, D., Llobet, E., Perez-Gutierrez, C., Tomas, J.M., *et al*. (2013) Role of bacterial surface structures on the interaction of *Klebsiella pneumoniae* with phagocytes. *PLoS ONE* **8:** e56847.

Marchetti, A., Mercanti, V., Cornillon, S., Alibaud, L., Charette, S.J., and Cosson, P. (2004) Formation of multivesicular endosomes in *Dictyostelium*. *J Cell Sci* **117:** 6053–6059.

Marchetti, A., Lelong, E., and Cosson, P. (2009) A measure of endosomal pH by flow cytometry in *Dictyostelium*. *BMC Res Notes* **2:** 7.

Melendez, A.J., and Tay, H.K. (2008) Phagocytosis: a repertoire of receptors and Ca(2+) as a key second messenger. *Biosci Rep* **28:** 287–298.

Mercanti, V., Charette, S.J., Bennett, N., Ryckewaert, J.J., Letourneur, F., and Cosson, P. (2006) Selective membrane exclusion in phagocytic and macropinocytic cups. *J Cell Sci* **119:** 4079–4087.

Monnat, J., Hacker, U., Geissler, H., Rauchenberger, R., Neuhaus, E.M., Maniak, M., and Soldati, T. (1997) *Dictyostelium discoideum* protein disulfide isomerase, an endoplasmic reticulum resident enzyme lacking a KDEL-type retrieval signal. *FEBS Lett* **418:** 357–362.

Nasser, W., Santhanam, B., Miranda, E.R., Parikh, A., Juneja, K., Rot, G., *et al*. (2013) Bacterial discrimination by dictyostelid amoebae reveals the complexity of ancient interspecies interactions. *Curr Biol* **23:** 862–872.

Pan, P., Hall, E.M., and Bonner, J.T. (1972) Folic acid as second chemotactic substance in the cellular slime moulds. *Nat New Biol* **237:** 181–182.

Peng, Z.L., Yang, J.Y., and Chen, X. (2010) An improved classification of G-protein-coupled receptors using sequence-derived features. *BMC Bioinformatics* **11:** 420.

Petersen, T.N., Brunak, S., von Heijne, G., and Nielsen, H. (2011) SignalP 4.0: discriminating signal peptides from transmembrane regions. *Nat Methods* **8:** 785–786.

Podschun, R., and Ullmann, U. (1998) *Klebsiella* spp. as nosocomial pathogens: epidemiology, taxonomy, typing methods, and pathogenicity factors. *Clin Microbiol Rev* **11:** 589–603.

Ravanel, K., de Chassey, B., Cornillon, S., Benghezal, M., Zulianello, L., Gebbie, L., *et al*. (2001) Membrane sorting in the endocytic and phagocytic pathway of *Dictyostelium discoideum*. *Eur J Cell Biol* **80:** 754–764.

Rifkin, J.L., and Goldberg, R.R. (2006) Effects of chemoattractant pteridines upon speed of *D. discoideum* vegetative amoebae. *Cell Motil Cytoskeleton* **63:** 1–5.

Sattler, N., Monroy, R., and Soldati, T. (2013) Quantitative analysis of phagocytosis and phagosome maturation. *Methods Mol Biol* **983:** 383–402.

Sengupta, P., Chou, J.H., and Bargmann, C.I. (1996) odr-10 encodes a seven transmembrane domain olfactory receptor required for responses to the odorant diacetyl. *Cell* **84:** 899–909.

Sigrist, C.J., Cerutti, L., de Castro, E., Langendijk-Genevaux, P.S., Bulliard, V., Bairoch, A., and Hulo, N. (2010) PROSITE, a protein domain database for functional characterization and annotation. *Nucleic Acids Res* **38:** D161–D166.

Sigrist, C.J., de Castro, E., Cerutti, L., Cuche, B.A., Hulo, N., Bridge, A., *et al*. (2013) New and continuing developments at PROSITE. *Nucleic Acids Res* **41:** D344–D347.

Sillo, A., Bloomfield, G., Balest, A., Balbo, A., Pergolizzi, B., Peracino, B., *et al*. (2008) Genome-wide transcriptional changes induced by phagocytosis or growth on bacteria in *Dictyostelium*. *BMC Genomics* **9:** 291.

Sroka, J., Madeja, Z., Michalik, M., Przestalski, S., and Korohoda, W. (2002) Folic acid, ascorbic acid and sodium selenite restore the motility of *Dictyostelium discoideum* inhibited by triethyllead. *Toxicology* **180:** 275–292.

Steinert, M. (2011) Pathogen-host interactions in *Dictyostelium*, *Legionella*, *Mycobacterium* and other pathogens. *Semin Cell Dev Biol* **22:** 70–76.

Tamura, K., Peterson, D., Peterson, N., Stecher, G., Nei, M., and Kumar, S. (2011) MEGA5: molecular evolutionary genetics analysis using maximum likelihood, evolutionary distance, and maximum parsimony methods. *Mol Biol Evol* **28:** 2731–2739.

Troemel, E.R., Chou, J.H., Dwyer, N.D., Colbert, H.A., and Bargmann, C.I. (1995) Divergent seven transmembrane receptors are candidate chemosensory receptors in *C. elegans*. *Cell* **83:** 207–218.

Underhill, D.M., and Gantner, B. (2004) Integration of Toll-like receptor and phagocytic signaling for tailored immunity. *Microbes Infect* **6:** 1368–1373.

Xiao, X., Wang, P., and Chou, K.C. (2009) GPCR-CA: a cellular automaton image approach for predicting G-protein-coupled receptor functional classes. *J Comput Chem* **30:** 1414–1423.

Supporting information

Additional Supporting Information may be found in the online version of this article at the publisher's web-site:

Fig. S1. Characterization of *fspA* KO cells. *fspA* KO cells obtained from the random mutagenesis screen had the REMI-mutagenic vector (pSC) inserted 98 nucleotides downstream from the start codon of DDB_G0277237 (A). To create by homologous recombination new *fspA* KO cells, we isolated the REMI vector with the genomic flanking sequences (obtained by digesting the genome with ClaI) and re-transfected it in WT cells. In (B), a schematic representation of the recovered KO plasmid cleaved at the ClaI site is shown: the vector comprises 2066 bp upstream from the BamHI insertion site (98 bp of *fspA* gene – depicted by a black box, plus 1968 bp upstream to *fspA* start codon – represented by a grey box) and 656 bp downstream; the pSC vector, containing the blasticidin resistance cassette, is in white.

Screen for KO cells was done by PCR using a combination of distinct pairs of oligonucleotides (C), allowing us to verify both gain and loss of signal in KO cells (D, E). Arrows in A and B indicate the position of the screening oligos.

Fig. S2. The organization of the endocytic pathway is unaltered in *fspA* KO cells.

A. Endosomal pH was determined as the fluorescence ratio of two internalized probes (pH-insensitive and pH-sensitive dextrans) at different chase times compared with a calibration curve. No significant difference was seen in acidification and neutralization of endosomal compartments between WT and *fspA* KO cells.

B. Recycling of fluid phase was measured in cells fed with Alexa-647 for 30 min, washed and chased for up to 180 min. Fluid phase remaining inside endosomal compartments was assessed in aliquots taken every 30 min. Internalized fluorescence at time 0 was defined as 100%, and no significant difference was observed between WT and *fspA* KO cells.

C. Phagosomal proteolysis was determined as the fluorescence ratio of DQG and Alexa-594 attached to the surface of latex beads. DQG is quenched when linked to the beads by BSA; degradation of BSA in the proteolytic phagosomal environment promotes the release and the de-quenching of DQG fluorescence. Alexa-594 shows no changes in fluorescence during the transit inside the phagosome. The fluorescence ratio in WT cells after 120 min was

defined as 100%, and no significant difference was seen in phagosome proteolysis between WT and *fspA* KO cells.
D. The enzymatic activity of lysosomal N-acetyl glucosaminidase was measured in the cellular lysate (intracellular) and in the cell culture medium (extracellular). Values were normalized to the total activity measured for WT cells; no significant difference was observed between WT and *fspA* KO cells.
E. Average speed of WT and *kil2* KO cells in the presence of *K. pneumoniae* and folate. No significant difference was observed between WT and *kil2* KO cells. $^{**}P < 0.01$, to control condition (in phosphate buffer).
Fig. S3. Presence of surface and internal markers in surface biotinylated fractions. To assess the amount of different markers in the surface biotinylated samples, one surface membrane protein (SibA) was used as positive control, and two internal proteins (cytoplasmic actin and ER-resident PDI) were used as negative controls. The Western blot of a representative experiment is shown; all lanes are from the same gel and have the same exposure time. For actin and PDI, 20% of the total biotinylated fraction volume was loaded, and dilutions of the lysate (from 0.025% to 0.005% of the total lysate volume) were used to estimate the amount of biotinylated proteins. For SibA, 2% of the total biotinylated fraction volume and 1% to 0.025% dilutions of the total lysate volume were loaded.
Table S1. Primers for semiquantitative RT-PCR.
Table S2. List of bacterial strains.
Table S3. UniProt accession numbers of the orthologues used for phylogenetic reconstruction (Fig. 2B).